Temporal Changes of CT Findings in 90 Patients with COVID-19 Pneumonia: A Longitudinal Study

Yuhui Wang, PhD[1,2,*], Chengjun Dong, MD[1,2,*], Yue Hu, PhD[3], Chungao Li, MD[1,2], Qianqian Ren, MD[1,2], Xin Zhang, MD[1,2], Heshui Shi, PhD[1,2], Min Zhou, PhD[1,2]

1 Department of Radiology, Union Hospital, Tongji Medical College, Huazhong University of Science and Technology, Wuhan, Hubei, China

2 Hubei Province Key Laboratory of Molecular Imaging, Wuhan, Hubei, China

3 Cancer Center, Union Hospital, Tongji Medical College, Huazhong University of Science and Technology, Wuhan, Hubei, China

*Y.W. and C.D. contributed equally to the manuscript.

Address correspondence to:

Min Zhou

1277 Jiefang Ave, Wuhan, Hubei, China 430022

E-mail: zhoumin_cmu@126.com

Manuscript Type: Original Research; Thoracic Imaging

Summary Statement

This prospective longitudinal study systematically described the temporal changes of CT findings in COVID-19 pneumonia and summarized the CT findings at the time of hospital discharge.

Key Results

The extent of CT abnormalities progressed rapidly after symptom onset, peaked during illness days 6-11, and followed by persistence of high levels.

The predominant pattern of abnormalities after symptom onset was ground-glass opacity; the percentage of mixed pattern peaked during illness days 12-17, and became the second most prevalent pattern thereafter.

Sixty-six of the 70 patients (94%) discharged had residual disease on final CT scans, with ground-glass opacity the most common pattern.

Abbreviations:

COVID-19: corona virus disease 2019

SARS-CoV-2: severe acute respiratory syndrome coronavirus 2

rRT-PCR: real-time reverse transcriptase-polymerase chain reaction

Abstract

Background: CT may play a central role in the diagnosis and management of COVID-19 pneumonia.

Purpose: To perform a longitudinal study to analyze the serial CT findings over time in patients with COVID-19 pneumonia.

Materials and Methods: During January 16 to February 17, 2020, 90 patients (male:female, 33:57; mean age, 45 years) with COVID-19 pneumonia were prospectively enrolled and followed up until they were discharged or died, or until the end of the study. A total of 366 CT scans were acquired and reviewed by 2 groups of radiologists for the patterns and distribution of lung abnormalities, total CT scores and number of zones involved. Those features were analyzed for temporal change.

Results: CT scores and number of zones involved progressed rapidly, peaked during illness days 6-11 (median: 5 and 5), and followed by persistence of high levels. The predominant pattern of abnormalities after symptom onset was ground-glass opacity (35/78 [45%] to 49/79 [62%] in different periods). The percentage of mixed pattern peaked (30/78 [38%]) on illness days 12-17, and became the second most predominant pattern thereafter. Pure ground-glass opacity was the most prevalent sub-type of ground-glass opacity after symptom onset (20/50 [40%] to 20/28 [71%]). The percentage of ground-glass opacity with irregular linear opacity peaked on illness days 6-11 (14/50 [28%)]) and became the second most prevalent subtype thereafter. The distribution of lesions was predominantly bilateral and subpleural. 66/70 (94%) patients discharged had residual disease on final CT scans (median CT scores and zones involved: 4 and 4), with ground-glass opacity (42/70 [60%]) and pure ground-glass opacity (31/42 [74%]) the most common pattern and subtype.

Conclusion: The extent of lung abnormalities on CT peaked during illness days 6-11. The temporal changes of the diverse CT manifestations followed a specific pattern, which might indicate the progression and recovery of the illness.

Introduction

The outbreak of coronavirus disease 2019 (COVID-19) originated in Wuhan China begins in December 2019 and has been lasting for more than 3 months(1). The disease quickly spreads across China and beyond, and as of March 8, 2020, a total of 105586 confirmed cases including 3584 deaths are reported worldwide(2).

CT plays a central role in the diagnosis and management of COVID-19 pneumonia (3). Previous efforts to analyze CT manifestations have continued. Some papers demonstrated the CT findings to be diverse, with the main abnormalities including ground-glass opacity and consolidation(4-6). Pan described the evolution of CT findings in 21 mild COVID-19 pneumonia patients(7). A better understanding of the progression of CT findings in COVID-19 pneumonia may help facilitate accurate diagnosis and disease stage. Thus, we performed a longitudinal study to analyze the serial CT findings in patients with COVID-19 pneumonia for temporal change.

Materials and Methods

This prospective observational study was approved by the Institutional Review Board of Union Hospital, Tongji Medical College, Huazhong University of Science and Technology. Informed consent was waived by the review board due to the observational nature of the study and the epidemic of COVID-19 as an emergency public health event.

Patients

Patients who were admitted to the isolation wards of Union Hospital with suspected COVID-19 pneumonia from January 16, 2020 to February 17, 2020, were screened using the following inclusion and exclusion criteria.

The inclusion criteria included: *(1)* at least 1 positive real-time reverse transcriptase-polymerase chain reaction (rRT-PCR) result for severe acute respiratory syndrome coronavirus 2 (SARS-CoV-2) in oropharyngeal swabs was obtained before or after admission; *(2)* at least 1 CT scan showed lung abnormalities before or after admission; *(3)* the electronic records were available. No specific excluding criteria were applied.

Treatment and Discharge Criteria

Treatment and discharge criteria for patients with COVID-19 pneumonia were in line with the Guidelines for the Diagnosis and Treatment of COVID-19 Pneumonia published by the National Health Commission of the People's Republic of China(3). The discharge criteria were specified as: *(1)* patients being afebrile

for at least 72 hours; *(2)* the respiratory symptoms significantly improving; *(3)* evidence of improvement on chest CT or radiograph; and *(4)* 2 consecutive negative SARS-CoV-2 rRT-PCR results at least 24 hours apart.

After admission, CT scans were at the discretion of the treating clinicians as appropriate for clinical scenario. We followed up the patients until they were discharged from hospital or died, or until the end of the study (March 8, 2020) if they were still in admission.

CT Protocol

Non-contrast chest CT scan was obtained with the patient in supine position, and scanning was performed at end inspiration. To minimize motion artifacts, patients were instructed on breath-holding. CT exams were done using multi-detector CT: Discovery 750HD (GE Medical Systems, Milwaukee, WI) and TOSHIBA Activion 16 (Toshiba, Tokyo, Japans). The scans were acquired and reconstructed as axial images using the following parameters: 1.25 mm section thickness, 1.25 mm interval, 120 kVp, and adaptive tube current. However, due to the large number of patients presenting for emergency CT scan and quick review, the following parameters were sometimes used on TOSHIBA Activion 16 for a faster transfer of images to PACS: 5 mm section thickness, 5 mm gap, 120 kVp, and adaptive tube current. Patients were assigned to whichever scanner that was available at the time of scan.

CT Image Interpretation

The CT scans before admission for each patient were also acquired for analysis.

Five experienced radiologists in 2 groups read the CT images (group one: YHW, CGL, and XZ, with an experience of 11, 12 and 3 years in radiology, respectively; group two: CJD and QQR, with an experience of 5 and 6 years in radiology, respectively). Multiple CT scans for a single patient were reviewed by the same group, and the decision was reached in consensus.

The main CT patterns were described in line with the terms defined by the Fleischner Society and peer-reviewed literature on viral pneumonia(8, 9). The CT images were assessed for the presence of ground-glass opacity (hazy areas of increased attenuation without obscuration of the underlying vasculature), consolidation (homogeneous opacification with obscuration of the underlying vasculature), reticular pattern (consisted of either coarse linear or curvilinear opacity or fine subpleural reticulation without substantial ground-glass opacity), mixed pattern (combination of consolidation, ground glass opacity and reticular opacity in the presence of architectural distortion) and honeycomb pattern. Furthermore, ground-glass opacity was subcategorized into: *(1)* pure ground-glass opacity; *(2)* ground-glass opacity with

smooth interlobular septal thickening; *(3)* ground-glass opacity with intralobular lines (crazy-paving pattern); and *(4)* irregular lines and interfaces with architectural distortion superimposed on ground-glass opacity. Examples of those patterns from our patient cohort were shown in Supplemental Figure E1 (Appendix E1). The distribution of abnormalities was also evaluated as predominantly subpleural (involving mainly the peripheral one-third of the lung), central (involving mainly the central two-third of the lung) or diffuse. Additionally, the presence of pleura effusion, pneumothorax, mediastinal emphysema, or mediastinal lymphadenopathy (axil diameter >1.0 cm) were also noted.

We quantified the CT images with a method published previously(9). Briefly, each lung was divided into 3 zones: upper (above the carina), middle, and lower (below the inferior pulmonary vein) zones; each zone was evaluated for percentage of lung involvement on a scale of 0-4 (0, 0% involvement; 1, less than 25% involvement; 2, 25% to less than 50% involvement; 3, 50% to less than 75%; 4, 75% or greater involvement). Overall CT scores was the summation of scores from all 6 lung zones. The maximum possible score was 24.

Statistical Analysis

Illness day 0 was defined as the day of initial symptom onset. The median values of total CT score and number of zones involved as a function of time were plotted. The temporal changes of main CT patterns, subtypes of ground-glass opacity, and the distribution of lung abnormalities were also analyzed. Kruskal-Wallis rank sum test was used for the difference between the median values of CT lung quantification in different period, and Chi-square test was applied to compare the frequency of CT patterns in different period. P value of < 0.05 was considered to be statistically significant. Statistical analyses were performed using R software (version 3.5.0, the R Foundation for Statistical Computing, Vienna, Austria).

Results

Patients

During January 16 to February 17, 2020, 107 patients were admitted to the isolation wards. Among them, 17 patients did not have a positive SARS-CoV-2 rRT-PCR result, resulting in a total of 90 patients enrolled in the final study. The median follow-up period was 18 days from admission (range: 5-43 days). The median illness duration from symptom onset to hospital discharge or death or the end of the study was 25 (range: 10-56).The demographic characteristics, initial symptoms and clinical outcomes were summarized in Table 1.

A total of 366 chest CT scans were acquired for the 90 patients. The numbers of CT scans in each day from symptom onset were listed in Supplementa1 Figure E2. Ten patients had their first CT scans before symptom onset (median days before symptom onset: 5, range 2 - 9 days) after they had close contact with suspected or confirmed COVID-19 patients. Each patient underwent a median of 4 scans (range: 1-7) with a median scan to scan interval of 6 days (range: 2-19 days). Thus, CT scans in every 6 days after symptom onset were categorized as one group for analysis. Of note, there were only 54 scans in total for illness days ≥ 24, and these scans were combined together and analyzed as one group.

Temporal Changes of CT Scores and Number of Zones Involved

Figure 1 showed the temporal changes of CT lung quantification. There were marked increase in the median values of total CT scores and number of zones involved after symptom onset. Both the median values of total CT scores and number of zones involved peaked during illness days 6-11, with the median values of 5 (interquartile range: 2-6, $p < 0.05$, compared to that of illness days 0-5) and 5 (2-6, $p < 0.05$), respectively. After that, the high levels persisted until illness days ≥ 24, and no significant changes were observed for both the median values of total CT scores and the number of zones involved ($p = 0.31$ and 0.76, respectively). The trends of both quantifications were similar to each other.

For total CT scores, the peak values were reached on median illness day 10 (interquartile range: 6-13). In 42/88 (48%) patients (2 patients died after the first CT scan), the total CT scores reached the peak values during illness days 6-11 (Figure 1C).

Temporal Changes of Main CT Patterns

Six of the 10 patients who had the first CT scans before symptom onset had normal CT scans. The other 4 patients had either ground-glass opacity (2 of 4 patients) or consolidation (2 of 4 patients). The period from the date of abnormal CT to that of the symptom onset ranged from 2 to 6 days.

The predominant pattern of abnormality after symptom onset was ground-glass opacity, with the percentage varying between 35/78 (45%) on illness days 12-17 to 49/79 (62%) on illness days 0-5 (Figure 2a). Consolidation was the second most prevalent finding during illness days 0-5 and 6-11, with the percentage of 18/79 (23%) and 20/85 (24%). Of note, 11/79 (14%) of CT scans during illness days 0-5, and 1/85 (1%) of CT scans during illness days 6-11 were normal, leading to an approximate sensitivity of utilizing CT for SARS-CoV-2 infection to be 53/63 patients (84%, 95% confidence interval: 73%-92%) and 74/75 patients (99%, 93%-100%) for each period.

The percentage of ground-glass opacity dropped significantly from 49/79 (62%) on illness days 0-5 to 35/78 (45%) on illness days 12-17 (p = 0.046), with a large increase in the percentage of mixed pattern from 1/79 (1%) to 30/78 (38%). The mixed pattern became the second most predominant pattern thereafter, with the percentage ranging from 12/54 (22%) on illness days ≥ 24 to 30/78 (38%) on illness days 12-17. The reticular pattern was rarely seen, and only present on illness days 18-23 and ≥ 24 with the percentage of 2/60 (3%) and 3/54 (6%), respectively.

Note that the percentage of ground-glass opacity showed gradual increase from 35/78 (45%) on illness days 12-17 to 33/54 (61%) on illness days ≥ 24, although the difference was not statistically significant (p = 0.097). To verify this upsurge in ground-glass opacity, patients with an illness duration ≥ 25 days from symptom onset (the median illness duration) were selected (48 patients with 204 CT scans) and the temporal changes of main CT patters had been shown in Supplemental Figure E3. Note that those patients contributed to 52/54 (96%) CT scans on illness days ≥ 24. A gradual increase from 14/36 (39%) on illness days 12-17 to 31/52 (60%) was also observed for the percentage of ground-glass opacity, although the difference was not statistically significant (p = 0.09).

Temporal Change of Ground-Glass Opacity

Only pure ground-glass opacity could be observed in CT scans before symptom onset (2 in 2 patients).

Pure ground-glass opacity was also the most commonly seen sub-type of ground-glass opacity after symptom onset, with the percentage ranging between 20/50 (40%) on illness days 6-11 to 20/28 (71%) on illness days 18-23 (Figure 2b). Ground-glass opacity with superimposed intralobular lines (crazy-paving pattern) were the second most commonly seen sub-type on illness days 0-5 with the percentage of 12/49 (24%). The percentage of irregular lines and interfaces superimposed on ground-glass opacity increased significantly from 4/49 (8%) on illness days 0-5 to 14/50 (28%) on illness days 6-11 (p = 0.02), and became the second most commonly seen pattern of ground-glass opacity thereafter.

Of note, the percentage of pure ground-glass opacity showed a trend of "first falling then rising". The percentage significantly dropped down from 32/49 (65%) on illness days 0-5 to 20/50 (40%) on illness days 6-11 (p = 0.02), with increase in the percentages of the other 3 subtypes. As the percentage significantly increased to 20/28 (71%, p = 0.02, as compared to that of illness days 6-11) on illness days 18-23 and 23/33 (70%, p = 0.02) on illness days ≥ 24, those of the other 3 patterns gradually decreased.

Three cases with series CT scans were shown in Figure 3-5.

Temporal Changes of the Distribution of CT Abnormalities

Fifteen of the 90 patients (17%) had lung lesions that were confined to a single lung throughout the course of the disease. Among them, 14 patients (93%) were discharged from hospital, and 4 (27%) had complete resolution of all abnormalities in the final CT scans at the end of the study. For the remaining 75 patients (303 CT scans), bilateral lesions were present in 257/303 (85%) of all CT scans. The temporal changes had been depicted in Supplemental Figure E4a. We can see that the unilateral involvement appeared only in the early and very last stage of the disease (illness days < 0, 0-5, 6-11, and ≥ 24), and the proportions gradually decreased with time after symptom onset from 18/66 (27%) on illness days 0-5 to 6/71 (12%) on illness days 6-11. All the lesions were bilateral on illness days 12-17 till 18-23.

In the 4 patients who had lung lesions before symptom onset, three had subpleural lesions (75%) and 1 had central lesions. The lung abnormalities were predominantly subpleural after symptom onset, with the percentage ranging from 36/54 (67%) on illness days ≥ 24 to 44/60 (73%) on illness days 18-23 (Supplemental Figure E4b). The percentage of diffuse pattern increased largely from 10/79 (13%) on illness days 0-5 to 25/85 (29%) on illness days 6-11, and remain relatively stable thereafter. The central distribution pattern was rarely seen after symptom onset, and only present on illness days 0-5, 6-11 and 12-17 with the percentages of 2/79 (3%), 1/85 (1%) and 1/78 (1%), respectively.

Other CT Findings

Six of 90 patients (7%) had mild bilateral pleural effusion. In 3 of them, pleural effusion was present during the entire course of the disease. Pleural effusion developed on illness days 11, 21, and 24 in the other 3 patients, and lasted till the last CT scans.

No pneumothorax, mediastinal emphysema, or mediastinal lymphadenopathy were observed on CT images.

CT Findings at the Time of Hospital Discharge

Seventy patients were discharged from hospital at the end of study. The median hospital stay was 16 days (range: 5-37 days), and the median illness days from symptom onset to discharge was 24 days (range: 10-44 days). The final CT scans were obtained at a median of 2 days (range: 0-8 days) before discharging. In 4 of the 70 patients, the last CT scans showed complete resolution of lung abnormalities. All the other 66 patients had residual disease on the last CT scans. The median values of CT scores and number of zones involved for all discharged patients were 4 (interquartile range: 2-6) and 4 (2-6), respectively. The distribution of the CT patterns was shown in Figure 6. Ground-glass opacity was the predominant abnormalities 42/70 (60%, 95% confidence interval: 48%-72%) found on the last CT scans, followed by a mixed pattern 17/70 (24%, 15%-36%). Pure ground-glass opacity was the most commonly seen subtype,

with the percentage of 31/42 (74%, 58%-86%). Ground-glass opacity with irregular lines and interfaces was noted in 8/42 (19%, 9%-34%) of all ground-glass opacity.

Discussion

In this study, we systematically depicted the longitudinal changes of CT findings in COVID-19 pneumonia. Our results suggested that the lung abnormalities increased quickly after the onset of symptoms, peaked around 6-11 days, and followed by persistence of high levels in extent for a long duration. Also, the diverse CT manifestations progressed in a specific pattern over time.

The CT findings of COVID-19 pneumonia reflected a typical lung injury of viral pneumonia, which characterized by a rapid change as seen in SARS and MERS(9-11). In our patient cohort, the peak levels of lung involvement were reached around 6-11 days from symptom onset, which was consistent with that of 10 days reported by Pan, and the time range of within the 2nd week as documented in SARS(7, 9). After that, persistence of high levels for both total CT scores and the zones involved were observed, indicating a slower absorption of COVID-19 pneumonia. It was similar to that reported in SARS(9). However, Pan showed a relatively faster decrease in CT scores after the peak, which might be because only patients with mild COVID-19 pneumonia were included(7).

The most common CT finding during the course of COVID-19 pneumonia in our patient cohort was ground-glass opacity alone. Consolidation was the second most seen feature in the first 11 days. When combining together, ground-glass opacity and consolidation constituted about 83% to 85% of all CT findings in total in the early stage of the disease. This was consisted with prior reports(5). The CT manifestations became more diverse during illness days 6-11 and later on. A mixed pattern with architectural distortion, mainly evolving from ground-glass opacity, became the second most predominant pattern since illness days 12-17. Of note, at least part of the mixed pattern characterized by perilobular abnormalities might suggest the presence of secondary organizing pneumonia, which needed to be confirmed with lung biopsy or bronchoalveolar lavage(12). Secondary organizing pneumonia resulting from viral pneumonia had been documented in SARS-CoV, MERS-CoV and influenza infections(13-15). Given that organizing pneumonia had the potential to progress to fibrosis and corticosteroid therapy was effective in the treatment, follow up CT scans might be needed to early identify suspected patients, especially those with typical CT manifestations (16, 17). Increase in Ground-glass opacity had been observed in late stages. The upsurge had also been shown in relatively severe patients with longer illness duration, although was not statistically significant. It might be due to the small sample size, and thus needed to be validated in a larger sample size. However, the upsurge in ground-glass opacity in late stages had also been seen in SARS(9). It might suggest that ground-glass opacity was the last stage of the illness

and the change of patterns to ground-glass opacity in late stage showed absorption or recovery of the illness.

For ground-glass opacity, pure ground-glass opacity was the most common subtype during the course of illness. Ground-glass opacity with superimposed irregular lines and interfaces was more commonly seen since illness days 6-11. This pattern could be mainly evolved from pure ground-glass opacity, and the linear opacity might be due to subsegmental atelectasis or secondary organizing pneumonia. The percentage of pure ground-glass opacity gradually and significantly increased from illness days 6-11, which could be accounted for by a decrease in the other 3 subtypes. This pattern change probably represent the gradual resolution of inflammation with reexpansion of alveoli, and thus indicate the absorption or recovery of illness.

Of note, two approximate sensitivities of 84% (95% confidence interval: 73%-92%) and 99% (93%-100%) were estimated for illness days 0-5 and 6-11, respectively. Those results indicated that the sensitivity of CT for SARS-CoV-2 infection increased over time after symptom onset, which was similar to prior reports(18). Several other studies had also reported the sensitivities, with the percentages varying from 44% to 98%(18-21). The difference between those sensitivities might be partly explained by the different duration from symptom onset to inclusion.

94% (66/70) of patients who were discharged from hospital at the end of the study still had mild to substantial residual lung abnormalities on their last CT scans. The main pattern of those lung abnormalities was ground-glass opacity. A most recent publication reported 4 discharged cases who had positive SARS-CoV-2 RT-PCR results again 5-13 days after discharging(22). Thus, follow-up monitoring of patients might still be necessary.

Of note, the data on illness days ≥ 24 was not always consistent with the trend as observed before illness days 24. A reasonable explanation was that the CT scans on illness days ≥ 24 were mainly from those patients with a longer illness duration, probably related to more severe illness.

There are several limitations in our study. First, subgroup analysis of mild and severe patients was not performed. Subgroup analysis would also be of great benefit in determining potential prognostic factors. Second, larger sample size and longer follow-up were needed to better depict the development of the illness.

In conclusion, the most commonly seen CT manifestations in COVID-19 pneumonia were bilateral ground-glass opacity with subpleural distribution and absence of pleural effusion. The extent of CT abnormalities progressed rapidly after the onset of symptoms, peaked around 6-11 days, and followed by

persistence of high levels in lung abnormalities. The temporal changes of the diverse CT manifestations followed a specific pattern, which might indicate the progression and recovery of the illness.

Reference

1. Li Q, Guan X, Wu P, Wang X, Zhou L, Tong Y, Ren R, Leung KSM, Lau EHY, Wong JY, Xing X, Xiang N, Wu Y, Li C, Chen Q, Li D, Liu T, Zhao J, Li M, Tu W, Chen C, Jin L, Yang R, Wang Q, Zhou S, Wang R, Liu H, Luo Y, Liu Y, Shao G, Li H, Tao Z, Yang Y, Deng Z, Liu B, Ma Z, Zhang Y, Shi G, Lam TTY, Wu JTK, Gao GF, Cowling BJ, Yang B, Leung GM, Feng Z. Early Transmission Dynamics in Wuhan, China, of Novel Coronavirus-Infected Pneumonia. The New England journal of medicine 2020. doi: 10.1056/NEJMoa2001316

2. WHO. https://www.who.int/emergencies/diseases/novel-coronavirus-2019/situation-reports/. (Accessed March 8. 2020).

3. National Health Commission of the People's Republic of China. The guidlines for the diagnosis and treatment of 2019-nCoV pneumonia (the 5th edition). Available at: *http://www.nhc.gov.cn/yzygj/s7653p/202002/d4b895337e19445f8d728fcaf1e3e13a/files/ab6bec7f93e64e7 f998d802991203cd6.pdf.* (Accessed March 8, 2020).

4. Pan Y, Guan H, Zhou S, Wang Y, Li Q, Zhu T, Hu Q, Xia L. Initial CT findings and temporal changes in patients with the novel coronavirus pneumonia (2019-nCoV): a study of 63 patients in Wuhan, China. European radiology 2020. doi: 10.1007/s00330-020-06731-x

5. Kanne JP. Chest CT Findings in 2019 Novel Coronavirus (2019-nCoV) Infections from Wuhan, China: Key Points for the Radiologist. Radiology 2020:200241. doi: 10.1148/radiol.2020200241

6. Heshui Shi XH, Nanchuan Jiang, Yukun Cao, Osamah Alwalid, Jin Gu, Yanqing Fan, Chuansheng Zheng. Radiological findings from 81 patients with COVID-19 pneumonia in Wuhan, China: a descriptive study. The Lancet Infectious Diseases 2020. doi: https://doi.org/10.1016/S1473-3099(20)30086-4

7. Pan F, Ye T, Sun P, Gui S, Liang B, Li L, Zheng D, Wang J, Hesketh RL, Yang L, Zheng C. Time Course of Lung Changes On Chest CT During Recovery From 2019 Novel Coronavirus (COVID-19) Pneumonia. Radiology 2020:200370. doi: 10.1148/radiol.2020200370

8. Hansell DM, Bankier AA, MacMahon H, McLoud TC, Muller NL, Remy J. Fleischner Society: glossary of terms for thoracic imaging. Radiology 2008;246(3):697-722. doi: 10.1148/radiol.2462070712

9. Ooi GC, Khong PL, Muller NL, Yiu WC, Zhou LJ, Ho JC, Lam B, Nicolaou S, Tsang KW. Severe acute respiratory syndrome: temporal lung changes at thin-section CT in 30 patients. Radiology 2004;230(3):836-844. doi: 10.1148/radiol.2303030853

10. Antonio GE, Ooi CG, Wong KT, Tsui EL, Wong JS, Sy AN, Hui JY, Chan CY, Huang HY, Chan YF, Wong TP, Leong LL, Chan JC, Ahuja AT. Radiographic-clinical correlation in severe acute respiratory syndrome: study of 1373 patients in Hong Kong. Radiology 2005;237(3):1081-1090. doi: 10.1148/radiol.2373041919

11. Das KM, Lee EY, Enani MA, AlJawder SE, Singh R, Bashir S, Al-Nakshbandi N, AlDossari K, Larsson SG. CT correlation with outcomes in 15 patients with acute Middle East respiratory syndrome coronavirus. AJR American journal of roentgenology 2015;204(4):736-742. doi: 10.2214/AJR.14.13671

12. Ujita M, Renzoni EA, Veeraraghavan S, Wells AU, Hansell DM. Organizing pneumonia: perilobular pattern at thin-section CT. Radiology 2004;232(3):757-761. doi: 10.1148/radiol.2323031059

13. Lai RQ, Feng XD, Gu YY, Lai HW, Liu F, Tian Y, Wang ZC, Zhang W, Chen GQ, Yang CH, Yang T. [Pathological changes of lungs in patients with severity acute respiratory syndrome]. Zhonghua bing li xue za zhi = Chinese journal of pathology 2004;33(4):354-357.

14. Ajlan AM, Ahyad RA, Jamjoom LG, Alharthy A, Madani TA. Middle East respiratory syndrome coronavirus (MERS-CoV) infection: chest CT findings. AJR American journal of roentgenology 2014;203(4):782-787. doi: 10.2214/AJR.14.13021

15. Gomez-Gomez A, Martinez-Martinez R, Gotway MB. Organizing pneumonia associated with swine-origin influenza A H1N1 2009 viral infection. AJR American journal of roentgenology 2011;196(1):W103-104. doi: 10.2214/AJR.10.4689

16. Kligerman SJ, Franks TJ, Galvin JR. From the radiologic pathology archives: organization and fibrosis as a response to lung injury in diffuse alveolar damage, organizing pneumonia, and acute fibrinous and organizing pneumonia. Radiographics : a review publication of the Radiological Society of North America, Inc 2013;33(7):1951-1975. doi: 10.1148/rg.337130057

17. Johkoh T, Muller NL, Cartier Y, Kavanagh PV, Hartman TE, Akira M, Ichikado K, Ando M, Nakamura H. Idiopathic interstitial pneumonias: diagnostic accuracy of thin-section CT in 129 patients. Radiology 1999;211(2):555-560. doi: 10.1148/radiology.211.2.r99ma01555

18. Bernheim A, Mei X, Huang M, Yang Y, Fayad ZA, Zhang N, Diao K, Lin B, Zhu X, Li K, Li S, Shan H, Jacobi A, Chung M. Chest CT Findings in Coronavirus Disease-19 (COVID-19): Relationship to Duration of Infection. Radiology 2020:200463. doi: 10.1148/radiol.2020200463

19. Guan WJ, Ni ZY, Hu Y, Liang WH, Ou CQ, He JX, Liu L, Shan H, Lei CL, Hui DSC, Du B, Li LJ, Zeng G, Yuen KY, Chen RC, Tang CL, Wang T, Chen PY, Xiang J, Li SY, Wang JL, Liang ZJ, Peng YX, Wei L, Liu Y, Hu YH, Peng P, Wang JM, Liu JY, Chen Z, Li G, Zheng ZJ, Qiu SQ, Luo J, Ye CJ, Zhu SY, Zhong NS, China Medical Treatment Expert Group for C. Clinical Characteristics of Coronavirus Disease 2019 in China. The New England journal of medicine 2020. doi: 10.1056/NEJMoa2002032

20. Fang Y, Zhang H, Xie J, Lin M, Ying L, Pang P, Ji W. Sensitivity of Chest CT for COVID-19: Comparison to RT-PCR. Radiology 2020:200432. doi: 10.1148/radiol.2020200432

21. Ai T, Yang Z, Hou H, Zhan C, Chen C, Lv W, Tao Q, Sun Z, Xia L. Correlation of Chest CT and RT-PCR Testing in Coronavirus Disease 2019 (COVID-19) in China: A Report of 1014 Cases. Radiology 2020:200642. doi: 10.1148/radiol.2020200642

22. Lan L, Xu D, Ye G, Xia C, Wang S, Li Y, Xu H. Positive RT-PCR Test Results in Patients Recovered From COVID-19. Jama 2020. doi: 10.1001/jama.2020.2783

Figures
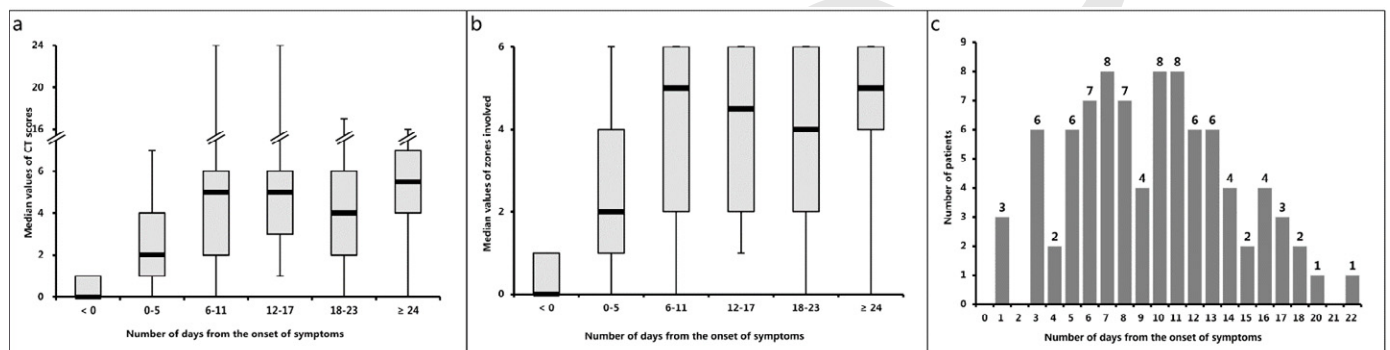
Figure 1. Temporal change of median values of total CT scores and number of zones involved. Both the median values of total CT scores (a) and number of zones involved (b) increased rapidly after symptom onset, peaked during illness days 6-11, and followed by persistence of high levels. The distribution of days when the peak total CT scores were reached was shown in (c). Note that 2 patients died after the first CT scan, resulting in a total of 88 peaking days.
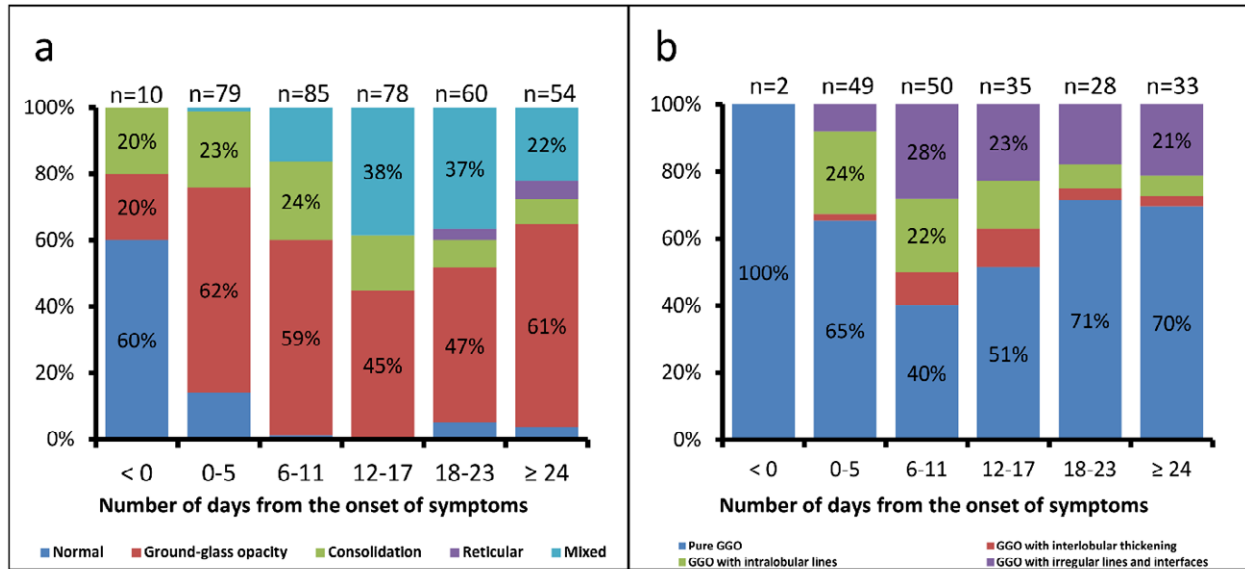
Figure 2. Temporal change of the main CT patterns and the subtypes of ground-glass opacity. Stacked-bar graphs showed the distribution of the main patterns of lung abnormalities (a) and the subtypes of ground-glass opacity (b) on CT scans at various time points from symptom onset. Categories with percentage ≥ 20% are shown. GGO = ground-glass opacity
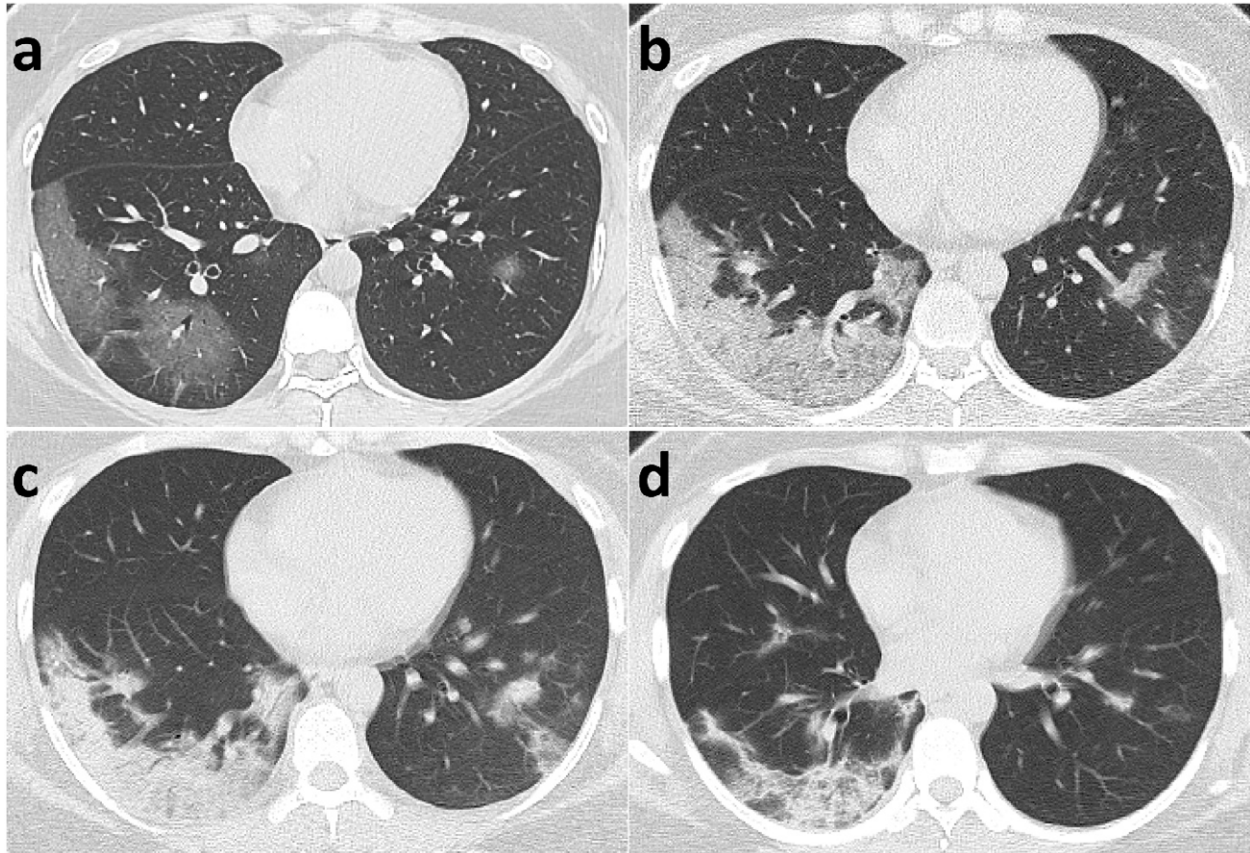
Figure 3. Series CT scans in 35-year-old woman with COVID-19 pneumonia. (a) Scan obtained on illness days 1 showed multiple pure ground-glass opacity (GGO) mainly in right lower lobe. (b) Scan obtained on illness days 5 showed increased extent of GGO and early consolidation. (c) Scan obtained on illness days 11 showed multiple consolidation with almost the same extent. (d) Scan obtained on illness days 15 showed a mixed pattern with a slightly smaller extent, and the perilobular consolidation might suggest the presence of organizing pneumonia. The patient was discharged on illness days 17.
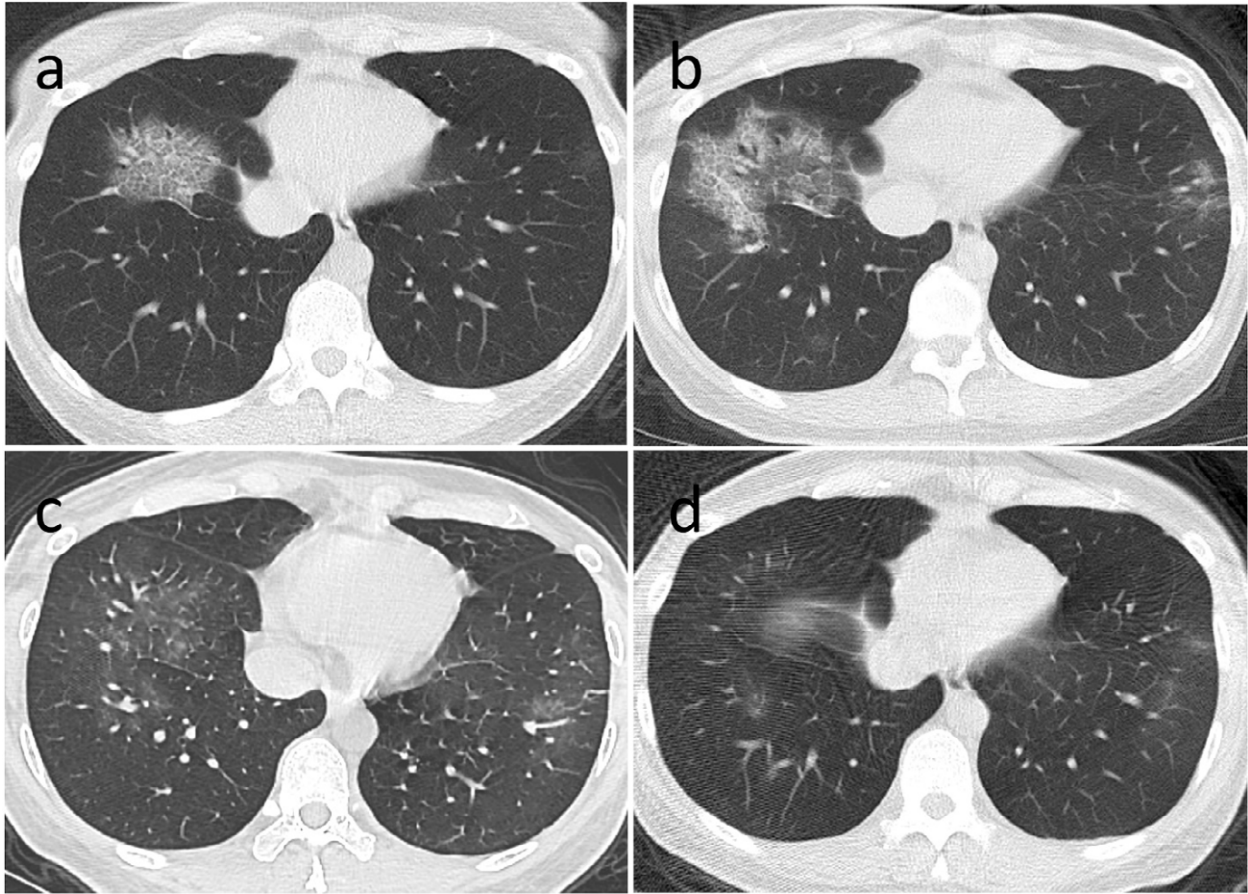
Figure 4. Series CT scans in a 41-year-old woman with COVID-19 pneumonia. (a) Scan obtained on illness days 3 showed ground-glass opacity with intralobular septal thickening (crazy-paving pattern) that affected right lower lobe. (b) Scan obtained on illness days 7 showed intralobular septal thickening superimposed on ground glass opacity with increased extent. Note that patchy ground-glass opacity newly developed in left lower lobe. (c) Scan obtained on illness days 12 showed absorption of abnormalities, with pure ground-glass opacity left in both lower lobes. (d) Scan obtained on illness days 17 showed obvious absorption of abnormalities. Only small pure ground-glass opacity could be observed in both lower lobes. The patient was discharged on illness days 20.
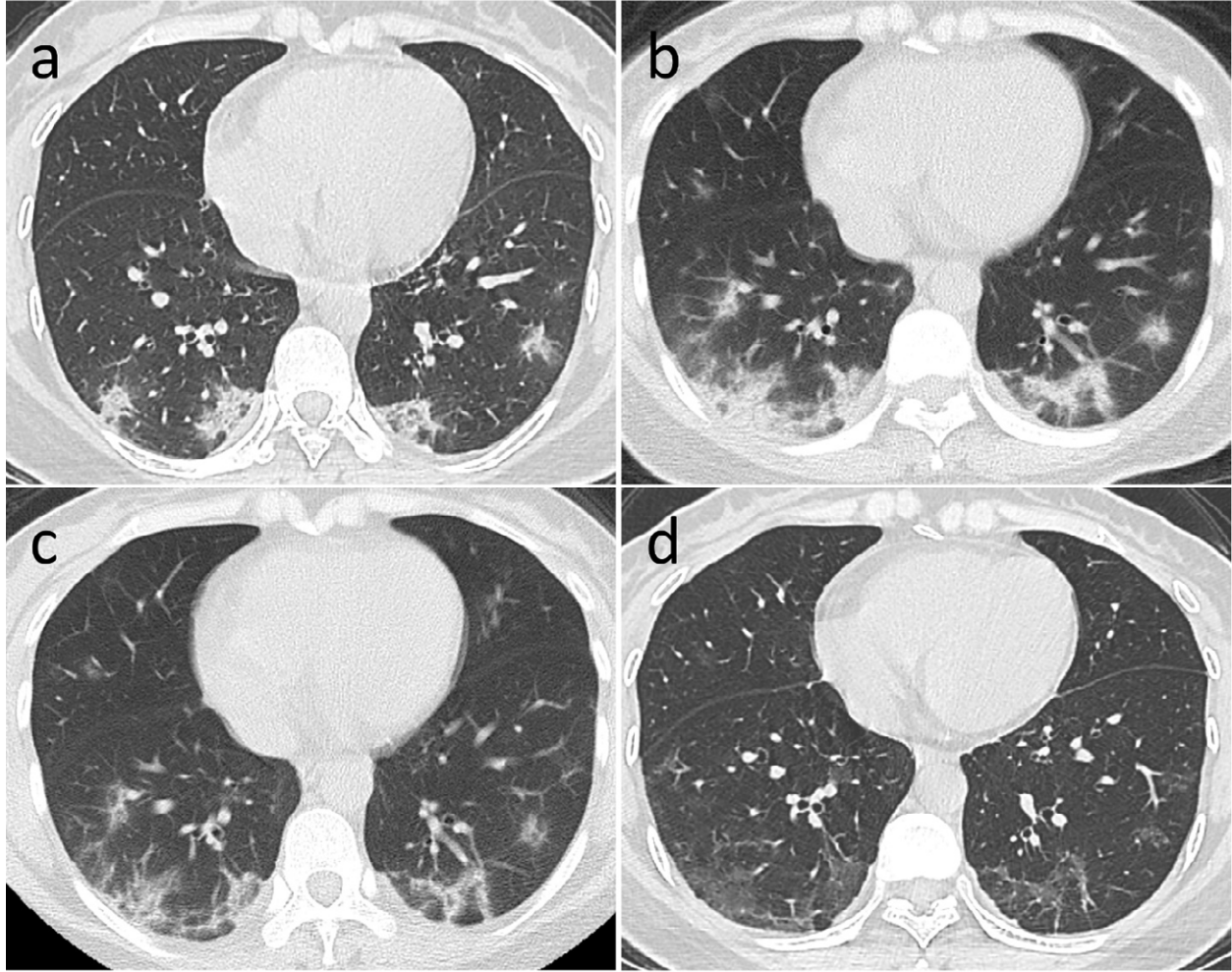
Figure 5. Series CT scans in a 38-year-old woman with COVID-19 pneumonia. (a) Scan obtained on illness days 8 showed small consolidation scattered in both lower lobes. (b) Scan obtained on illness days 13 showed consolidation with increased extent. (c) Scan obtained on illness days 19 showed a mixed pattern with bandlike consolidation and parenchymal bands in both lower lobes. The perilobular bands of consolidation suggested the possible presence of organizing pneumonia. (d) Scan obtained on illness day 25 showed pure ground-glass opacities with almost the same extent. The patient was discharged on illness days 30.
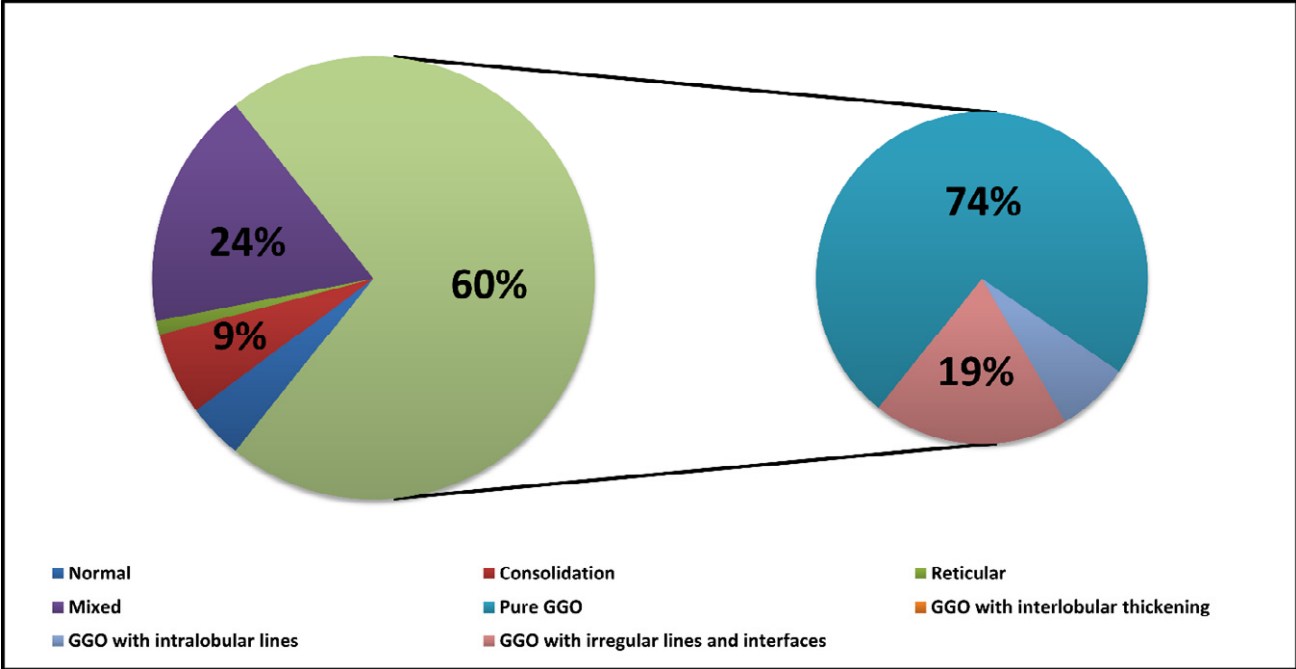
Figure 6. The distribution of CT patterns of the final CT scans at the time of hospital discharge in 70 patients. GGO = ground-glass opacity.

Table. The demographic characteristics, initial symptoms and clinical outcomes of the included patients

Age, gender, initial symptoms and clinical outcomes	Number of patients (Percentage)
Age (y, mean ± standard deviation)	45 ± 14
Gender (male : female)	33 : 57
Initial symptoms	
Fever	55 (61%)
Hypodynamia	22 (24%)
Cough	20 (22%)
Chest tightness	8 (9%)
Sore throat	7 (8%)
Chills	7 (8%)
Diarrhea	6 (7%)
Anorexia	6 (7%)
Headache	4 (4%)
Muscle pain	4 (4%)
Bellyache	2 (2%)
Clinical outcomes at the end of study	
Discharged	70 (78%)
In admission	17 (19%)
Died	2 (2%)
Transferred to other hospitals	1 (1%)